**Preprints.org**

Article

# A Comparative Study of Stem Rot Severity in Mature Deciduous Trees in Latvia

Jānis Liepiņš [*] , Kaspars Liepiņš , Andis Lazdiņš , Roberts Matisons , Āris Jansons

*Article*

# A Comparative Study of Stem Rot Severity in Mature Deciduous Trees in Latvia

**Jānis Liepiņš \*, Kaspars Liepiņš, Andis Lazdiņš, Roberts Matisons and Āris Jansons**

Latvian State Forest Research Institute "Silava", Rigas Street 111, LV-2169 Salaspils, Latvia

\* Correspondence: janis.liepins@silava.lv

**Abstract:** Efforts to enhance carbon storage in forest ecosystems through policy and management decisions rely on accurate forest biomass assessments. However, most forest inventories consider tree mortality the only form of aboveground biomass loss, overlooking other important factors, such as wood decay in living trees. In this study, using linear mixed-effects models, we delve into the sustainability of mature and over-mature deciduous forests in Latvia by conducting a comprehensive analysis of stem rot severity, identifying species for which the impact of stem rot on their carbon stock reduction was most significant. The analysis focused on determining the proportion of discolored wood, decomposed wood, and hollow spaces within the stems of 190 living deciduous trees commonly found in hemiboreal forests. The study reveals a greater extent of stem rot and more extensive decay in *Populus tremula* trees than in *Betula* spp., *Alnus glutinosa*, and *Alnus incana*. It emphasizes the influence of tree species, age, and diameter at breast height on stem rot proportions. The stump rot area significantly predicts the amount of decomposed and discolored wood within the stem. The study provides valuable insights for sustainable forestry practices and highlights challenges in estimating stem rot severity, emphasizing the need for comprehensive diagnostic methods.

**Keywords:** internal decay; stem quality; discoloration; old forests; tree cavities; decay assessment; resource management; political ecology

## 1. Introduction

Forests are expected to be crucial in making Europe the first climate-neutral continent by 2050 [1] while coping with biodiversity loss. The European Union (EU) has established ambitious targets to address climate change and promote sustainability, recognizing forests as a crucial component of these efforts. Old-growth forests described by various structural attributes [2] are extremely valuable for protecting biodiversity and providing many ecosystem services [3]. Strictly protecting the remaining primary and old-growth forests is a major target of the EU Biodiversity Strategy. However, the foreseen rise in protected forest areas has triggered a debate about the influence of such action on forests as carbon pools [4–6]. A comprehensive knowledge of carbon accumulation dynamics in different forest ecosystems over different maturity stages is essential in evaluating the long-term impact of various forest management decisions and protection scenarios.

The forest age structure is essential for understanding its current functioning and development and predicting the dynamics of future carbon sinks under changing climate conditions for the long-term removal of carbon dioxide ($CO_2$) from the atmosphere [7,8]. Stem rot, a ubiquitous and natural phenomenon in forests, deteriorates tree vitality over time and mainly affects the lower parts of older trees [9–11]. This process releases carbon from the wood to the atmosphere, causing a significant but poorly quantified carbon flux [12,13]. Most existing data about stem rot spatial distributions in forests originates from research investigations examining its impact on the quantity and value of timber [14–16]. However, to track the impact of stem rot on carbon stocks in living biomass, more precise and comprehensive data are needed on the extent and proportion of various external indicators of stem rot within tree stems [17].

According to 2022 National Forest Inventory (NFI) data, birch (*Betula* spp.), European aspen (*Populus tremula* L.), grey alder (*Alnus incana* L. Moench), and common alder (*Alnus glutinosa* L. Gaertn.) cover 51.8% of total forest areas and account for 44.7% of standing timber in Latvia. The

proportional distribution of these tree species is comparable to that found in other Baltic States [18]. Over the last decade, the area of mature and old-growth broadleaved forests in Latvia has increased by approximately 5% and is expected to grow further to fulfill the goals of the EU Biodiversity Strategy for 2030. Given the limited extent of remaining primary and old-growth forests in Europe, the strategy emphasizes the establishment of additional forest areas to expand the network of protected areas, thereby meeting the target for strict protection [19].

The assumption that old-growth forests are carbon-neutral has been long-standing. Mature and old-growth forests function as carbon sinks, accumulating carbon over extended periods, often spanning centuries [4,20,21]. For instance, among the most prevalent deciduous tree species, old-growth birch and aspen stands store more total ecosystem carbon than old-growth pine and spruce stands in hemiboreal forests [22]. However, the impact of hearth rot on forest carbon has rarely been evaluated [23–25]. In the context of changing forest age structure, effective solutions to enhance the comprehension of decay column biomass estimations and how stem rot severity varies under different tree and stand characteristics within mature and over-mature forests remain scarce. Given the heightened emphasis on natural climate solutions and the necessity to assess the tradeoffs between forest carbon and conventional management objectives, readily available data on accurate stocks and rates represent a vital resource for guiding the development of management plans and gauging the potential of the forest carbon sink.

Significant distinctions exist between the decay processes occurring in living stems and those in deadwood—i.e., fallen and standing dead trees—a subject that has been extensively studied on global and regional scales [26–29]. Decay development in a living stem can be likened to a disease, and the tree can often respond to the initial infection and defend itself [30]. In our previous fieldwork, we observed a significant decline in basic stem wood density (25%–41%) as part of decomposition [17]. This variation depended on the tree species and was associated with biomass loss in tree stems. Previous studies, especially those conducted in old-growth forests, might have systematically overestimated tree biomass carbon by not considering internal decay.

The traditional assessment of tree stem vitality typically involves visual inspection, core drilling, and other nondestructive testing techniques that allow evaluation of the internal health status of trees without causing damage [30,31]. Studies that quantify the decay severity by evaluating the difference in the decay degree and its spatial patterns, particularly regarding vertical distribution, have been notably limited, especially in mature and old-growth forests, as the destructive sampling (felling of trees) is labor-intensive and often impossible in older forests due to various restrictions and constraints.

This research aims to bridge the gap in baseline information regarding trends in the severity of stem rot in hemiboreal mature and over-mature deciduous forests and identify stands where the impact of stem rot on carbon stock reduction could be the most significant. We sought to answer the following research questions:

1.  What variations exist in stem rot severity among different mature deciduous species?
2.  How does the severity of individual stem rot change in relation to tree characteristics within a stand?
3.  In which species might the impact of rot on aboveground biomass be most significant?

## 2. Materials and Methods

### 2.1. Study Area

Latvia is situated in Eastern Europe, bordering the Baltic Sea, within the hemiboreal forest zone, between the temperate deciduous forests and the boreal coniferous forests [32]. This transitional region is a relatively narrow belt and exhibits features resembling boreal forests. However, it stands out due to a slightly greater tree species diversity and a climate characterized by higher moisture levels and moderate coolness. The study was conducted in 32 mature and over-mature forest stands located in sites managed by the Forest Research Station (Figure 1), facilitating the organization of tree-cutting activities. To characterize the forest stands (Table 1), circular plots with an area of 500 m²

were intentionally positioned within each stand, chosen to best represent the overall characteristics of the stand. These stands represented the four most prevalent broadleaved tree species in Latvia: birch (*Betula pendula* Roth. and *Betula pubescens* Ehrh., not distinguished in Latvian forest inventory), European aspen (*Populus tremula* L.), grey alder (*Alnus incana* L. Moench), and common alder (*Alnus glutinosa* L. Gaertn.).
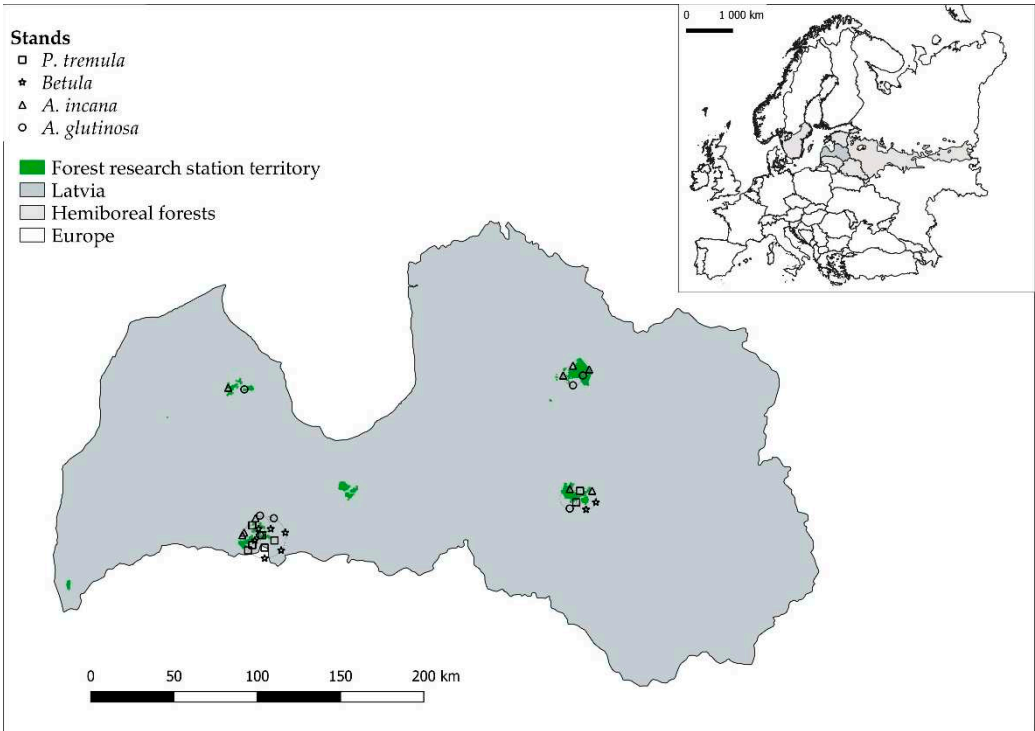


**Figure 1.** Study site, located within forests of the Forest Research Station (green).

**Table 1.** Characteristics of the assessed stands, categorized by dominant species. The range is shown in parentheses.

| Dominant species | Number of stands | Age, years | Diameter at breast height, cm | Tree height, m | Number of dominant trees, ha$^{-1}$ | Proportion of decayed trees, % |
|---|---|---|---|---|---|---|
| *Betula* | 8 | 85.5 (69–109) | 25.5 (20.9–29.9) | 24.0 (19.9–28.4) | 455 (340–620) | 31.6 (11.8–100) |
| *P. tremula* | 8 | 81.8 (69–110) | 39.2 (30.1–55.2) | 32.8 (27.8–38.1) | 230 (140–320) | 61.2 (10.0–100) |
| *A. glutinosa* | 7 | 89.8 (65–122) | 27.8 (20.6–32.6) | 24.8 (22.7–26.7) | 600 (240–900) | 38.6 (6.7–93.3) |
| *A. incana* | 9 | 48.1 (37–70) | 21.0 (17.0–31.0) | 21.5 (18.1–24.4) | 860 (420–1260) | 27.7 (2.4–81.0) |

All the dominant tree species' stems were horizontally drilled at the stump level from three directions using the Rinntech RESISTOGRAPH® R650 for stem rot detection. This nondestructive method is reliable for assessing the presence of rot [31,33], enabling the evaluation of changes in wood density caused by internal decay by measuring drilling resistance. A tree was classified as decayed if a decrease in density (Figure 2) was detected in at least one of the drilling directions or if at least one conk was found on the stem. The appearance of a conk represents a significant heart rot and is often caused by various stem decay fungi [30]. The trees identified as decayed were marked and subsequently felled to measure the decay extent. The tree stump's height was determined as 1% of the total tree height before felling.
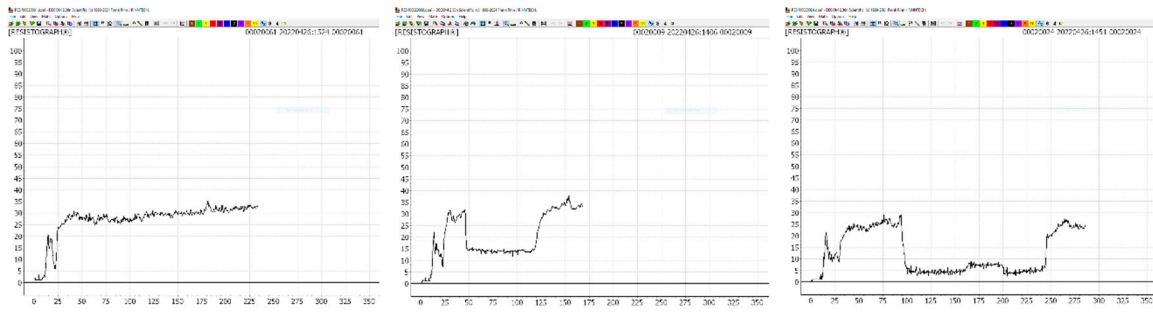
4

**Figure 2.** Example of drilling profiles. The left one represents a healthy tree, the middle one depicts advanced rot, and the right one represents a hollow tree. The X-axis displays drilling depth (mm), and the Y-axis represents relative drilling resistance (%).

## 2.2. Data Collection

Data were obtained from destructively sampled trees. The tree stems were cross-cut into 1-m logs from the stem base to the tree top. The presence of stem rot was evaluated by visually inspecting the logs at their ends and at 1.3 m high. Stem discs were collected from the affected logs if signs of stem rot, such as discoloration, decomposed wood, or hollow, were observed. Two discs were obtained from each log, one from each end, and the percentage of stem rot was measured according to previously defined external decay indicators [17]:

- Discolored wood: includes wood that has experienced discoloration but retains most of its mechanical properties, with only minor changes.
- Decomposed wood: comprises wood that has undergone decomposition to the extent that it can be squeezed between two fingers, indicating a significant loss of structural integrity.
- Hollow: refers to wood with a hollow interior, signifying substantial decay and the presence of a void or empty space within the tree stem.

The height of stem rot was measured by dividing the last stem section into smaller portions using 10-cm intervals, allowing for a detailed examination of the spatial distribution and progression of decay along the tree stem. All stem discs were scanned, and on each disc, diameters in two perpendicular directions and areas of discoloration, decomposed wood, and hollow spaces were manually measured using ImageJ software (National Institutes of Health, Bethesda, MD, USA) (Figure 3). The values obtained from ImageJ were calibrated using a ruler in each image.

The volume of stem rot in logs—between two sample discs—was calculated using Smalian's approach:

$$V_{Si} = \frac{L_{Si}(g_{1i} + g_{2i})}{2} \tag{1}$$

Where $V_{Si}$ is the stem rot volume (discolored, decomposed, or hollow) in log section $i$ (m³), $L_{Si}$ is the length of the log section containing stem rot $i$ (cm), $g_{1i}$ is the lower surface's cross-sectional area of stem rot in section $i$ (mm²), and $g_{2i}$ is the upper surface's cross-sectional area of stem rot in section $i$ (mm²). If only one of the log ends exhibits stem rot and the other has sound wood or a different wood condition, we assume that the stem rot has a conical shape, with its base on the visible end and its tip on the other end—meaning that the stem rot area decreases linearly from one end to the other. In this case, the length of the cone is equal to the actual length of stem rot in section $i$. The total decayed, decomposed, or hollow wood volume was calculated at the tree level by summing each tree's log volumes.
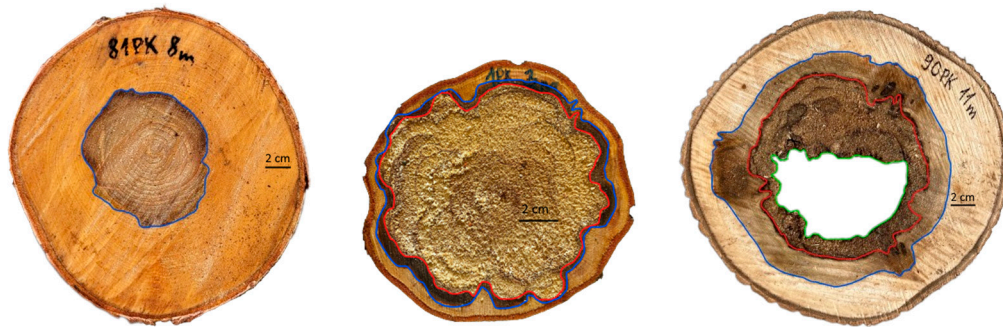
**Figure 3.** Measurement of the area of discoloration (blue), decomposed wood (red), and hollow space (green) in stem cross-section discs.

Finally, we computed the decay proportion of trees with a stem rot. It is expressed as the ratio of decayed wood volume to the tree's total volume and conveys how much of the tree's wood quality and value is reduced by fungal decay. The stem volume functions employed in the Latvian NFI are used to calculate the individual tree volumes for the study species [34]. In mixed stands of > 40-year-old *B. pendula* and *B. pubescens*, morphological characteristics may fail to correctly identify the species. This study used a chemical method based on the presence of a phenolic compound called platyphylloside in the inner bark of *B. pendula*, and its hybrids were used to distinguish between these two species using destructively sampled trees [35]. However, the species were analyzed together due to insufficient observations.

*2.3. Data Analysis*

The statistical analyses were performed in R v. 4.1.3 [36]. We employed linear mixed-effects models using the "lme4" package to investigate the impact of stand age, tree diameter at breast height (DBH), and tree height (H) on total rot, discolored wood, decomposed wood, and hollow proportions. The tree species (factorial with four levels), age, DBH, and H (numeric covariates), and their interaction were considered fixed effects. We employed sites as a random effect, assuming random slopes and intercepts for the tested fixed effects, to address unbalanced data and prevent pseudoreplication issues [37],

The influence of tree stump diameter and total stump rot area on the proportions of discolored wood, decomposed wood, and hollows was assessed similarly using separate linear mixed-effects models. An analysis of deviance tables with Type II Wald $\chi^2$ tests was constructed for these models using the "Anova" function in the R "car" package. We evaluated the adherence of the models to statistical assumptions through diagnostic plots. Predictor effect plots were generated using the "effects" package to visualize the significant predictors.

We calculated the conditional $R^2$ (variance explained by the full model) and marginal $R^2$ (variance explained by fixed effects) using the package "MuMIn."

**3. Results**

*3.1. Stem Rot Incidence in Mature Stands*

The incidence of advanced stem rot at the stump level was higher in investigated *P. tremula* stands than in the other studied deciduous species common in hemiboreal and boreal forests (Table 1). The average rot incidence in the examined *P. tremula* trees was 61.2%, with a wide variation across individual stands from 10% to 100%. In contrast, the *Betula*, *A. incana*, and *A. glutinosa* forests had a lower incidence, approximately half that of *P. tremula*, averaging 27.7%–38.6% depending on the species. Out of the 190 trees examined with stem rot, 162 (85%) exhibited advanced rot, and 53 (28%) displayed hollowness on the stump surface. In certain trees, discoloration was only evident at the stump level, while decomposed wood or hollow were observed higher up in the tree stem. These

observations suggest that decay symptoms may not always originate at the tree's base and can manifest at different heights. This pattern was particularly pronounced in *P. tremula*, for which out of 24 trees displaying hollowness, the presence of a hollow on the stump was visible in only 11 trees (< 50%) (Table 1).

### 3.2. Stem Rot Severity and Variability Across Tree Species

Characteristics of sampled trees and their stem rot are summarized in Table 2. The total length of decay in the felled stems varied between species, ranging from 9.9 ± 5.7m for *Betula* to 19.3 ± 5.5m for *P. tremula*, on average. While the axial extent of the hollow between the studied species displayed minimal variation, the length of the decomposed wood column for *P. tremula* was significantly greater, averaging 15.0 ± 6.5 m. These results starkly contrasted with other species, where the length of decomposed wood ranged only from 1.1 to 2.7 m. The total diameter of decay at the stump level did not exhibit significant variations across the examined tree species. The stump-level decay diameter exhibited a significant positive correlation ($p < 0.001$) with parameters like DBH (r = 0.56–0.78) and stump diameter (r = 0.58–0.79), indicating a robust association between tree dimensions and increased decay area at the stump level across studied species.

The mean stem volume for the examined species ranged from 0.3 m³ for *A. incana* to 1.7 m³ for *P. tremula*, with the corresponding stem rot volumes ranging from 0.09 to 0.57 m³, respectively (Figure 4). The average proportion of total stem rot was the lowest in *Betula* trees, at approximately 15.5%, suggesting that *Betula* trees generally exhibit a lower extent of decay than the other studies species, such as *A. glutinosa*, *A. incana*, and *P. tremula*. These species exhibit higher decay proportions, with averages ranging from 20.1% for *A. glutinosa* to 31.9% for *P. tremula*. However, noting the substantial variability within each species is crucial. Individual trees may significantly deviate from these average values, indicating a broad range of decay proportions within each species. This variability underscores the complexity of biological systems and the influence of various environmental and genetic factors on the decay process.
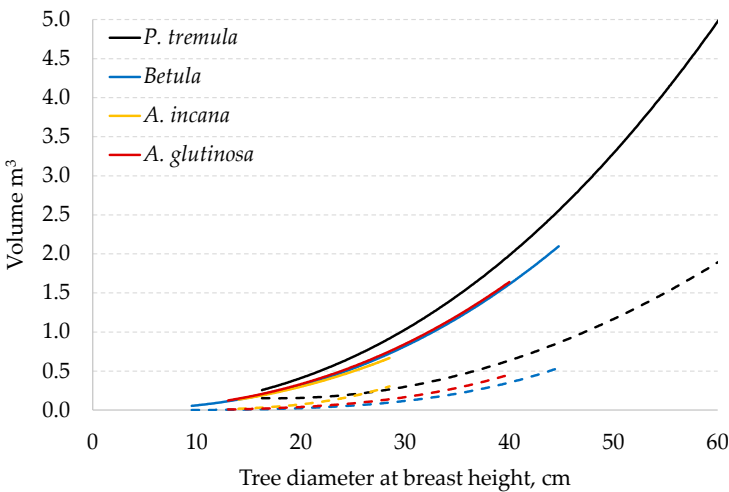


**Figure 4.** Stem volume (solid line) and stem rot volume (dashed line) in sampled trees.

**Table 2.** Tree characteristics and metrics of internal stem defects of sampled trees

| Parameters | *Betula* (*N* = 60) | | *P. tremula* (*N* = 60) | | *A. incana* (*N* = 38) | | *A. glutinosa* (*N* = 32) | |
|---|---|---|---|---|---|---|---|---|
| | Mean ±SD | Range | Mean±SD | Range | Mean±SD | Range | Mean±SD | Range |
| Tree H, m | 23.9±3.9 | 13.1–31.8 | 32.0±3.7 | 18.7–39.3 | 20.8±2.4 | 16.3–26 | 23.3±3.1 | 11.9–28.5 |
| Tree DBH, cm | 25.1±6.5 | 9.5–44.7 | 35.8±10.3 | 16.25–65.0 | 19.3±3.5 | 14.0–28.5 | 23.9±6.7 | 13.0–40.0 |

| | | | | | | | | |
|---|---|---|---|---|---|---|---|---|
| Stem volume, m⁻³ | 0.6±0.3 | 0.1–2.1 | 1.7±1.1 | 0.2–5.7 | 0.3±0.1 | 0.1–0.7 | 0.6±0.4 | 0.1–1.7 |
| Total length of decay, m | 9.9±5.7 | 1.1–23.6 | 19.3±5.5 | 5.2–27.9 | 10.7±4.5 | 2.2–18.2 | 11.5±4.8 | 1.4–18.8 |
| Length of decomposed wood column, m | 2.5±2.8 | 0.2–13.9 | 15.0±6.5 | 3.5–27.2 | 1.1±1.1 | 0.3–5.5 | 2.7±3.3 | 0.4–13.2 |
| Lenght of hollow column, m | 1.1±1.0 | 0.2–3.9 | 1.4±1.4 | 0.1–6.5 | 0.7±0.2 | 0.5–1.2 | 1.3±0.9 | 0.4–2.8 |
| Total diameter of decay at stump level, cm | 13.8±6.3 | 2.7–29.7 | 20.9±11.5 | 4.25–58 | 14.2±4.0 | 8.0–19.5 | 13.9±6.1 | 4.8–25.5 |
| Diameter of decomposed wood at stump level, cm | 11.5±5.7 ($N$ = 49) | 1.2–27.5 | 14.3±8.0 ($N$ = 51) | 1.25–39.7 | 13.1±4.8 ($N$ = 34) | 3.5–23.5 | 13.3±6.1 ($N$ = 28) | 3.8–29.0 |
| Diameter of hollow at stump level, cm | 11.4±4.8 ($N$ = 27) | 3.7–21.0 | 12.1±7.7 ($N$ = 11) | 1–30.5 | 8.7±2.9 ($N$ = 7) | 5.3–14.5 | 10.3±6.2 ($N$ = 8) | 3.8–23.8 |
| Total decay proportion (% of volume) | 15.5±11.4 | 0.5–47.3 | 31.9±12.6 | 4.8–58.5 | 28.5±16.7 | 3.7–57.6 | 20.1±12.3 | 0.8–46.1 |
| Decomposed wood proportion (% of volume) | 3.6±4.9 ($N$ = 58) | 0.01–18.2 | 16.3±7.6 ($N$ = 60) | 2.91–36.7 | 6.4±8.3 ($N$ = 36) | 0.2–40.8 | 6.3±6.8 ($N$ = 31) | 0.2–31.6 |
| Hollow proportion (% of volume) | 1.7±1.8 ($N$ = 30) | 0.1–7.9 | 0.8±0.8 ($N$ = 24) | 0.01–3.6 | 1.5±1.8 ($N$ = 7) | 0.2–5.8 | 1.7±1.7 ($N$ = 8) | 0.1–4.4 |

### 3.3. Effect of Tree Characteristics on Rot Amount

The analysis of the deviance table using Type II Wald $\chi^2$ tests indicated significant fixed effects on the response variables, particularly the total rot proportion. Additionally, the discoloration and decomposed wood proportions were individually significantly influenced. Notably, the species factor exhibited the most significant main effect on total stem rot proportion ($\chi^2$ = 50.5, $p < 0.001$), followed by the stand age ($\chi^2$ = 16.7, $p < 0.001$) (Table 3). These results suggest that different tree species have different levels of rot susceptibility in terms of color and structure changes. Moreover, the species-age and species-DBH interactions also displayed substantial effects, signifying that the relationship between these factors and the decay proportions varies among tree species (Figure 5). In contrast, tree H and its interactions with the other factors did not significantly affect ($p > 0.05$) the stem rot proportions in mature and over-mature trees. Neither the variables, including species, age, DBH, and H, nor their interactions were statistically significant ($p > 0.05$) in influencing the tree hollow proportion.

The analysis of the species-age interaction effects (Figure 5A–C) revealed that stand age primarily affects the total rot proportion in *P. tremula* and *A. incana* stems. The impact of age on the proportion of discolored wood varies among tree species. Specifically, *A. incana* exhibits a notable rise (from 10% to 40%) in its discolored wood proportion with aging (40–70 years old), whereas *P. tremula* displays a significant increase in its decomposed wood proportion instead, from 10% to 30% in 70–110-year-old stands. No significant changes in discolored or decomposed wood proportions were observed in *A. glutinosa* and *Betula* trees. At the stand level, the tree DBH significantly characterizes the total rot proportion of *P. tremula* ($p$ = 0.033) and *Betula* ($p$ = 0.006) trees (Figure 5D). In *P. tremula* stands, this phenomenon is due to the decreasing proportion of decomposed wood in stems with increasing DBH. In contrast, in *Betula* stands, the total proportion of stem volume affected by rot increases for larger trees, mainly as the discolored wood proportion increases.

**Table 3.** Analysis of deviance table (Type II Wald $\chi^2$ tests) for the linear mixed-effects model to investigate the effect of species, age, DBH, and H on the various proportions of stem volume affected by rot: total rot, discolored wood, decomposed wood, and hollow. The table shows the $\chi^2$ statistic and significance level for each term in the model. Numbers in bold represent statistical significance. A colon denotes the interactions between the fixed effects.

| Fixed effects | Response variables | | | |
|---|---|---|---|---|
| | Total rot | Discolored wood | Decomposed wood | Hollow |

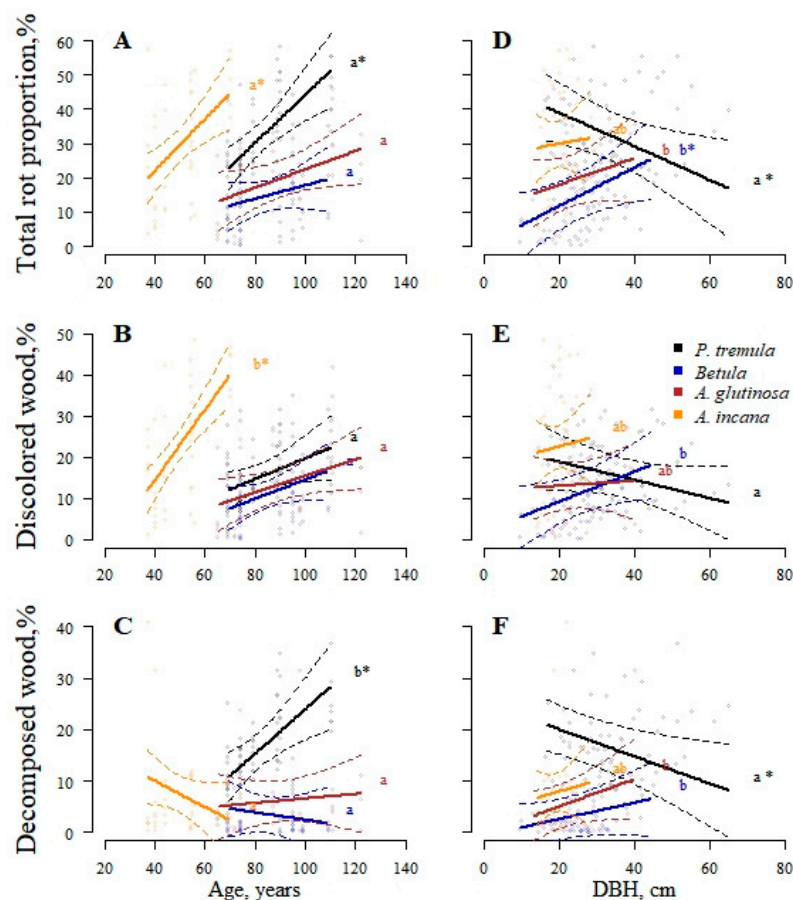| Species | 50.5***[1] | 44.3*** | 41.2*** | 0.8 |
|---|---|---|---|---|
| Age | 16.7*** | 20.2*** | 1 | 0.7 |
| DBH | 0.5 | 2.5 | 0.1 | 0.1 |
| H | 0.1 | 2.4 | 3.4 | 0.5 |
| Species:Age | 13.2** | 13.0** | 23.9*** | 0.3 |
| Species:DBH | 8.9* | 5.3 | 7.5* | 0.3 |
| Species:H | 2.3 | 3.4 | 1.8 | 0.9 |
| | | | | |
| Conditional $R^2$ | 0.57 | 0.49 | 0.75 | 0.25 |
| Marginal $R^2$ | 0.46 | 0.37 | 0.50 | 0.18 |

$***p < 0.001, **p < 0.01, *p < 0.05$



**Figure 5.** Effect plots displaying variation in stem volume proportions affected by rot among different tree species and age (A–C) or DBH (D–F). These variations correspond to the significant interaction effects presented in Table 3. The area between dotted lines indicates a 95% confidence interval. Different letters indicate significant differences between species, and asterisks denote significant effects of age or DBH on stem rot proportion.

### 3.4. Effect of Stump Characteristics on Rot Amount

Stump diameter displayed a significant main effect on decomposed wood ($\chi^2 = 3.9$, $p < 0.05$) but did not exhibit a significant effect on discolored wood ($\chi^2 = 1.5$, $p = 0.22$) or hollow spaces ($\chi^2 = 1.0$, $p = 0.32$) (Table 4). This result suggests that larger stumps tend to have a greater loss of stem volume due to advanced rot. Rot area on the stump surface significantly affected discolored wood ($\chi^2 = 19.4$, $p < 0.001$) and decomposed wood ($\chi^2 = 17.2$, $p < 0.001$) but not hollow ($\chi^2 = 0.3$, $p = 0.62$), implying that

the extent of rot on the stump surface was positively correlated with the amounts of discolored and decomposed wood within the stem.

We observed significant interactions between species and stump diameter for discolored wood and between species and stump rot area for discolored and decomposed wood. These interactions indicate that the effects of stump diameter and stump rot area on the stem volume proportions affected by rot were inconsistent across studied tree species. No significant interactions were found for hollow ($p > 0.05$ for all tests), suggesting that the proportion of hollow stem volume did not depend on stump parameters or their combinations with species.

The proportion of wood affected by stem rot, measured as the stump rot area, significantly predicts the amount of decomposed and discolored wood in the stem. This effect varies depending on the tree species, with *Betula*, *A. incana*, and *A. glutinosa* displaying a significant relationship between rot area and decomposed wood and *Betula* and *A. incana* exhibiting a significant correlation between rot area and discolored wood (Figure 6). In summary, the decomposed wood model has the highest explanatory power for fixed factors alone (marginal $R^2$) and for fixed and random factors combined (conditional $R^2$), followed by the discolored wood model. As the models indicate, a significant portion of the variance in the stem volume proportions affected by rot is attributed to random factors, such as the stand characteristics. This observation suggests that stand-specific factors are crucial in determining the extent of rot in stem volumes.

**Table 4.** Analysis of deviance table (Type II Wald $\chi^2$ tests) for the linear mixed-effects model to investigate the effect of species, stump rot area, and stump diameter on the stem volume proportions affected by rot: discolored wood, decomposed wood, and hollow. The table indicates the $\chi^2$ statistic and significance level for each term in the model. Numbers in bold are statistically significant. A colon denotes the interactions between the fixed effects.

| Fixed effects | Response variables | | |
|---|---|---|---|
| | Discolored wood | Decomposed wood | Hollow |
| Species | **9.1*[1]** | **26.6*** | 3.4 |
| Stump diameter | 1.5 | **3.9*** | 1.0 |
| Stump rot area | **19.4*** | **17.2*** | 0.3 |
| Species:Stump diameter | **9.1*** | 4.7 | 0.5 |
| Species:Rot area on stump | **17.5*** | **40.1*** | 0.3 |
| | | | |
| Conditional $R^2$ | 0.58 | 0.83 | 0.17 |
| Marginal $R^2$ | 0.22 | 0.35 | 0.10 |

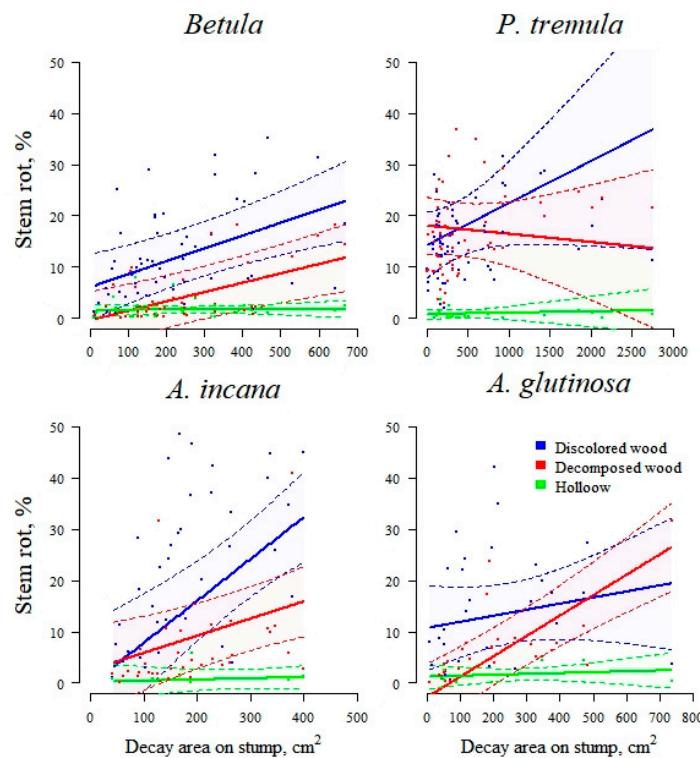***$p < 0.001$, **$p < 0.01$, *$p < 0.05$

**Figure 6.** Effect plots displaying the relationships between the proportions of discolored wood, decomposed wood, and hollow stem volume affected by rot and the total stump rot area. The area between the dotted lines represents a 95% confidence interval, while the asterisks indicate statistically significant effects of the stump rot area on the rot proportions.

## 4. Discussion

Evaluating the impacts of stem rot is crucial, given the decreased tree vitality and biomass in mature and over-mature deciduous stands, which is driven by environmental stressors and aging. Our sampling design was not intended to generate valid models for predicting the severity of rot in damaged trees that could be incorporated into existing forest carbon accounting methodologies. We were interested in discovering the extent of the influence of various tree characteristics on the severity of stem rot to enhance our understanding of the complex dynamics of forest ecosystems and provide valuable insights for future research in modeling biomass losses caused by internal stem decay.

### 4.1. Stem Rot Incidence and Variability Across Tree Species

According to a study by Johansson [38], 91% of the 12–63 year-old *P. tremula* stems examined in southern Sweden exhibited discoloration signs, a clear indication of fungal decay. *Populus* spp. have been characterized by Shigo [10] as "poor wound compartmentalizers," a trait that could partially account for the high prevalence (58.8%) of decay observed in these species in the USA and Canada [11]. In Latvia, reliable data on stem rot incidence within *P. tremula* forest stands is lacking. Our research findings confirm that a substantial proportion of trees (61.2%) among the studied *P. tremula* stands are affected by advanced decay, consistent with other studies. Interestingly, unlike other deciduous species, the presence of decomposed wood was not always visible on the surface of aspen stumps. However, the consistent visibility of discolored wood served as a reliable indicator of stem rot presence. These observations underscore the complexity of diagnosing advanced rot based solely on external observations and highlight the need for more comprehensive diagnostic methods.

Stem rot is common for *A. incana* trees in Latvian forests, affecting 18% of the trees and varying widely (1%–54%) among stands [39]. This finding is consistent with previous research on gray alder in Finland, which reported even higher decay frequency and variation among stands [40]. According

to a different study, *A. glutinosa* stands exhibit a greater prevalence of decay than *A. incana*, with rates ranging from 53% to 98% across various mature stands [41]. This difference implies that *A. glutinosa* is more vulnerable to heart rot than *A. incana*, highlighting the varying susceptibilities of these tree species to internal stem decay. *Alnus* species, particularly *A. incana*, are characterized by relatively short lifespans, rendering them susceptible to stem decay, particularly in mature stands [39,41,42]. Research in the Baltic region has highlighted that middle-aged gray alder stands tend to function as carbon sinks, while mature stands transition into carbon sources, underscoring the complex role of these species in the carbon cycle within forest ecosystems [43]

According to a study by Hynynen et al. [44], silver birch (*B. pendula*) has a lower decay incidence than other boreal tree species, such as *P. tremula*, *A. glutinosa*, *A. incana*, and *P. abies*. However, decay and discoloration may differ greatly among *Betula* spp. and with management practices, such as pruning—which increases the probability of wood staining [45]. For instance, discoloration in stem pith was most common at a relative height of 2.5%, where about 75% to 100% of the trees exhibited discoloration signs [16]. This study's data further supports the observation that *B. pubescens* tends to exhibit a higher incidence of internal stem decay than *B. pendula* stands, potentially due to its shorter life cycle. Out of the 60 *Betula* trees randomly selected for the study, only 11 were *B. pendula*, and the majority were *B. pubescens*. This distribution could indicate a higher prevalence of stem rot in *B. pubescens* trees. The most recent study by Buht et al. [46] has confirmed variations in biomass allocation patterns among *Betula* species, emphasizing the need for further research to determine the prevalence of stem rot in each species.

The difference in decay occurrence may be related to each species' different wood properties and susceptibility to fungal infection. Detecting incipient decay and discolored wood in trees at stump height using drilling resistance devices is challenging and sometimes deemed impossible [31,47]. This difficulty may result in underestimating the number of decayed trees within the studied stands. Moreover, advanced decay may not be present at stump height, especially for aspens, where spores can enter through broken branch stubs [48]. Therefore, the true decay incidence in the studied stands may be higher than observed in this study.

### 3.2. Challenges Faced in Predicting Stem Rot Severity

The total proportion of stem volume affected by rot in *Betula*, *P. temula*, *A. glutinosa*, and *A. incana* trees primarily increased with stand age. Notably, this increasing trend differed among the tree species and the discolored or decomposed wood sections, as evidenced by the significant species-age interaction effect (Table 3 and Figure 5). Older stands are also more susceptible to rot infection, consistent with previous studies [15,25,49]. Some deciduous tree species might exhibit greater susceptibility to stem rot at comparable ages, while others may be more resistant. Considering the tree species' distinct biological aging cycles is critical, as it may impact their susceptibility or resistance to stem rot. For instance, *A. incana* is known for its rapid growth and distinctly shorter life span than the other species under study [50]. This difference emphasizes the importance of considering tree age and species when developing models to predict stem rot severity.

Understanding how patterns of stem rot infection vary with tree size is critical for assessing its influence on forest biomass estimation, especially considering that the largest trees in the stand contribute the most to the aboveground biomass [25]. We initially anticipated that tree size, characterized by variables like DBH and H, would have a substantial explanatory capacity in predicting stem rot proportions in mature and over-mature stands. However, the fixed effects analysis (Table 3) revealed that H and its respective interactions did not significantly affect stem rot proportions. In contrast to H, thinner *P. tremula* trees exhibited a significantly higher proportion of decomposed wood, suggesting their higher susceptibility to stem rot than larger trees. This observation suggests that, while tree size was not the primary influential factor, other variables like species and age played a more critical role in predicting the severity of stem rot in mature and over-mature stands.

Apart from *P. tremula*, at stand level, the proportion of decomposed wood in *Betula*, *A. incana*, and *A. glutinosa* stems significantly correlates with the stump rot area (Figure 6), suggesting that this

parameter will also be strongly correlated with stem biomass losses. The average proportion of decomposed wood in *P. tremula* is 16.3% ± 7.6%, more than twice as high as in the other studied species. Predicting the advanced rot in *P. tremula* stems is challenging as the stump surface does not always reliably indicate highly progressive internal decay (Figure 7). This idea is further supported by the wide data dispersion observed during the analysis of rot proportion in *P. tremula* stems.



**Figure 7.** Patterns of decay associated with rot infection in *P. tremula* stems. On the left, a well-developed rot is visible at stump height. On the right, there is a widespread rot in the upper part of the stem.

Assessing the internal condition of standing trees is challenging because rot can be hidden, progressive, and sometimes located in the stems' upper parts. Visual and drilling decay evaluation techniques may not be reliable or accurate for detecting progressive rot unless combined with expensive technologies, such as tomography. The resolution of conventional tomographic techniques is often sufficient to accurately capture discoloration and advanced rot within tree stems [24,51]. Drilling at breast height or stump level can be dependable to identify trees with substantial rot sections [14]. Measuring the longitudinal extent of internal decay within a tree's stem can be another challenge, as standard methods may not easily accomplish this. A more accurate approach involves measuring the decay after felling the tree, which was adopted in this study. This understanding is crucial in comprehending decay dynamics since the actual level of decay in a standing tree is influenced by both the species' decay resistance and the variations in decay occurrence at different heights.

*3.3. Importance of Stem Rot in Tree Biomass Estimations*

One major concern affecting the use of broadleaved trees, particularly *Populus* spp., is the presence of wood decay and discoloration, even in relatively young and small trees [48]. Although we observed a significant proportion (15.5%–31.9%) of stem volumes affected by rot in the studied tree species in mature and over-mature stands (Table 2), it is important to note that not all stem rot leads to biomass and carbon losses. A notable decrease in wood basic density, accompanied by increased wood nitrogen content, occurs within the stem wood during decomposition. *Betula* exhibited the most substantial reduction in density due to stem rot (mean difference between discolored and decomposed wood = 0.196 g m$^{-3}$), followed by *P. tremula* (0.152 g m$^{-3}$), *A. incana* (0.132 g m$^{-3}$), and *A. glutinosa* (0.102 g m$^{-3}$) [17]. This decrease (25%–41%) corresponded to the biomass loss in the decomposed wood volume. No significant changes in wood properties were observed at the early decay stage, as the basic density of discolored wood was very similar to the average density of intact wood reported for the same tree species in previous studies [52–58]. Tree hollows were mainly

confined to the lower one meter of the tree stems, accounting for approximately 1.5% of the stem volume. Therefore, their existence is likely to have a negligible impact on the overall losses in stem biomass.

While stem rot is recognized as a source of error in forest aboveground biomass estimates, only a few studies attempted to evaluate the effect of stem rot on biomass or carbon losses. Using data from 3180 drilled, felled, and cored stems in mixed dipterocarp forests, stem rot was estimated to reduce total forest aboveground biomass by up to 7% relative to what would be predicted, assuming all stems are composed strictly of intact wood [14]. In old-growth oak forests, internal stem decay was detected in 6% of the trees, resulting in only a marginal overestimation of stand biomass by about 1% [25]. Findings from another study indicated that internal decay in trees resulted in an estimated carbon loss ranging from 0.13% to 36.7% in the lower boles, emphasizing the impact of decay on carbon stocks within forest ecosystems [24]. A study conducted in urban forests revealed that decayed wood can potentially decrease carbon storage by an estimated range of 69–110 kg per tree across four studied species in Australia [12]. Additionally, the observed volume loss ranged from 0.17 to 0.75 m³, corresponding to 5%–25% of the stem volume.

As the comprehension of stem rot incidence in hemiboreal forests increases, future studies should focus on developing stand-level models to evaluate the impact of rot on biomass or carbon reduction. Incorporating stem rot information into forest planning enables better management and climate protection strategies, such as identifying rot-prone areas, mitigating rot effects, and prioritizing tree species for planting or preservation.

## 5. Conclusions

Damage from stem rot in living trees represents an underappreciated component of the forest carbon cycle, and its significance is expected to increase with tree age. This study underscores the considerable intra- and inter-species variability in the severity and extent of stem rot. Furthermore, it identifies potential covariates for future investigations. The results indicate that mature and over-mature *P. tremula* trees tend to exhibit higher decay rates, especially advanced rot, than the other studied tree species. Consequently, given the high incidence and severity of rotten trees, potential biomass losses due to stem rot emerge as a significant factor when considering the preservation of old stands dominated by *P. tremula* for climate protection. To ensure the sustainability of these ecosystems, forest management strategies should include thorough assessments of stem rot severity, considering the possible trade-offs, especially in relation to biodiversity and carbon storage goals.

**Author Contributions:** Conceptualization, J.L. and K.L.; methodology, J.L.; formal analysis, Ā.J. and A.L.; writing—original draft preparation, J.L. and K.L.; writing—review and editing, J.L.; visualization, J.L. and R.M.; supervision, A.L.; project administration, Ā.J.; funding acquisition, Ā.J. All authors have read and agreed to the published version of the manuscript."

**Data Availability Statement:** Data available on request from the corresponding author.

**Conflicts of Interest:** The authors declare no conflict of interest.

## References

1.    Lier, M.; Köhl, M.; Korhonen, K.T.; Linser, S.; Prins, K.; Talarczyk, A. The New EU Forest Strategy for 2030: A New Understanding of Sustainable Forest Management? *Forests* 2022, *13*.

2.    Bauhus, J.; Puettmann, K.; Messier, C. Silviculture for Old-Growth Attributes. *For. Ecol. Manage.* **2009**, *258*, 525–537, doi:https://doi.org/10.1016/j.foreco.2009.01.053.

3.   DellaSala, D.A.; Mackey, B.; Norman, P.; Campbell, C.; Comer, P.J.; Kormos, C.F.; Keith, H.; Rogers, B. Mature and Old-Growth Forests Contribute to Large-Scale Conservation Targets in the Conterminous United States. *Front. For. Glob. Chang.* **2022**, *5*, doi:10.3389/ffgc.2022.979528.

4.   Luyssaert, S.; Schulze, E.-D.; Börner, A.; Knohl, A.; Hessenmöller, D.; Law, B.E.; Ciais, P.; Grace, J. Old-Growth Forests as Global Carbon Sinks. *Nature* **2008**, *455*, 213–215, doi:10.1038/nature07276.

5.   Gundersen, P.; Thybring, E.E.; Nord-Larsen, T.; Vesterdal, L.; Nadelhoffer, K.J.; Johannsen, V.K. Old-Growth Forest Carbon Sinks Overestimated. *Nature* **2021**, *591*, E21–E23, doi:10.1038/s41586-021-03266-z.

6.   Luyssaert, S.; Schulze, E.-D.; Knohl, A.; Law, B.E.; Ciais, P.; Grace, J. Reply to: Old-Growth Forest Carbon Sinks Overestimated. *Nature* **2021**, *591*, E24–E25, doi:10.1038/s41586-021-03267-y.

7.   Yang, H.; Ciais, P.; Frappart, F.; Li, X.; Brandt, M.; Fensholt, R.; Fan, L.; Saatchi, S.; Besnard, S.; Deng, Z.; et al. Global Increase in Biomass Carbon Stock Dominated by Growth of Northern Young Forests over Past Decade. *Nat. Geosci.* **2023**, *16*, 886–892, doi:10.1038/s41561-023-01274-4.

8.   Vilén, T.; Gunia, K.; Verkerk, P.J.; Seidl, R.; Schelhaas, M.-J.; Lindner, M.; Bellassen, V. Reconstructed Forest Age Structure in Europe 1950–2010. *For. Ecol. Manage.* **2012**, *286*, 203–218, doi:https://doi.org/10.1016/j.foreco.2012.08.048.

9.   Seifert, T. Simulating the Extent of Decay Caused by Heterobasidion Annosum s. l. in Stems of Norway Spruce. *For. Ecol. Manage.* **2007**, *248*, 95–106, doi:10.1016/j.foreco.2007.02.036.

10.  Shigo, A.L.; Hillis, W.E. Heartwood, Discolored Wood, and Microorganisms in Living Trees. *Annu. Rev. Phytopathol.* **1973**, *11*, 197–222, doi:10.1146/annurev.py.11.090173.001213.

11.  Frank, J.; Castle, M.E.; Westfall, J.A.; Weiskittel, A.R.; Macfarlane, D.W.; Baral, S.K.; Radtke, P.J.; Pelletier, G. Variation in Occurrence and Extent of Internal Stem Decay in Standing Trees across the Eastern US and Canada: Evaluation of Alternative Modelling Approaches and Influential Factors. *Forestry* **2018**, *91*, 382–399, doi:10.1093/forestry/cpx054.

12.  Orozco-Aguilar, L.; Johnstone, D.; Livesley, S.J.; Brack, C. The Overlooked Carbon Loss Due to Decayed Wood in Urban Trees. *Urban For. Urban Green.* **2018**, *29*, 142–153, doi:10.1016/j.ufug.2017.09.008.

13.  Barba, J.; Bradford, M.A.; Brewer, P.E.; Bruhn, D.; Covey, K.; van Haren, J.; Megonigal, J.P.; Mikkelsen, T.N.; Pangala, S.R.; Pihlatie, M.; et al. Methane Emissions from Tree Stems: A New Frontier in the Global Carbon Cycle. *New Phytol.* **2019**, *222*, 18–28, doi:10.1111/nph.15582.

14.  Heineman, K.D.; Russo, S.E.; Baillie, I.C.; Mamit, J.D.; Chai, P.P.K.; Chai, L.; Hindley, E.W.; Lau, B.T.; Tan, S.; Ashton, P.S. Evaluation of Stem Rot in 339 Bornean Tree Species: Implications of Size, Taxonomy, and Soil-Related Variation for Aboveground Biomass Estimates. *Biogeosciences* **2015**, *12*, 5735–5751, doi:10.5194/bg-12-5735-2015.

15.  Schneider, R.; Riopel, M.; Pothier, D.; Côté, L. Predicting Decay and Round-Wood End Use Volume in Trembling Aspen (Populus Tremuloides Michx.). *Ann. For. Sci.* **2008**, *65*, 608–608, doi:10.1051/forest:2008042.

16.  Hallaksela, A.M.; Niemistö, P. Stem Discoloration of Planted Silver Birch. *Scand. J. For. Res.* **1998**, *13*, 169–176, doi:10.1080/02827589809382973.

17.  Liepiņš, J.; Jaunslaviete, I.; Liepiņš, K.; Jansone, L. Effect of Stem Rot on Wood Basic Density, Carbon, and Nitrogen Content of Living Deciduous Trees in Hemiboreal Forests. *Silva Fenn.* **2023**, *57*.

18.  Rytter, L.; Johansson, K.; Karlsson, B.; Stener, L.G. Tree Species, Genetics and Regeneration for Bioenergy Feedstock in Northern Europe. In *Forest BioEnergy Production: Management, Carbon Sequestration and Adaptation*; 2013; pp. 7–37 ISBN 9781461483915.

19.  Hermoso, V.; Carvalho, S.B.; Giakoumi, S.; Goldsborough, D.; Katsanevakis, S.; Leontiou, S.; Markantonatou, V.; Rumes, B.; Vogiatzakis, I.N.; Yates, K.L. The EU Biodiversity Strategy for 2030: Opportunities and Challenges on the Path towards Biodiversity Recovery. *Environ. Sci. Policy* **2022**, *127*, 263–271, doi:https://doi.org/10.1016/j.envsci.2021.10.028.

20.  Hoover, C.M.; Smith, J.E. Aboveground Live Tree Carbon Stock and Change in Forests of Conterminous United States: Influence of Stand Age. *Carbon Balance Manag.* **2023**, *18*, 7, doi:10.1186/s13021-023-00227-z.

21.  Fraser, J.S.; Pile Knapp, L.S.; Graham, B.; Jenkins, M.A.; Kabrick, J.; Saunders, M.; Spetich, M.; Shifley, S. Carbon Dynamics in Old-Growth Forests of the Central Hardwoods Region, USA. *For. Ecol. Manage.* **2023**, *537*, 120958, doi:https://doi.org/10.1016/j.foreco.2023.120958.

22.  Ķēniņa, L.; Elferts, D.; Jaunslaviete, I.; Bāders, E.; Šņepsts, G.; Jansons, Ā. Tree Biomass – a Fragile Carbon Storage in Old-Growth Birch and Aspen Stands in Hemiboreal Latvia. *Balt. For.* **2022**, *28*, 156–165, doi:10.46490/BF654.

23.  Matsuzaki, E.; Sanborn, P.; Fredeen, A.L.; Shaw, C.H.; Hawkins, C. Carbon Stocks in Managed and Unmanaged Old-Growth Western Redcedar and Western Hemlock Stands of Canada's Inland Temperate Rainforests. *For. Ecol. Manage.* **2013**, *297*, 108–119, doi:10.1016/j.foreco.2012.11.042.

24.  Marra, R.E.; Brazee, N.J.; Fraver, S. Estimating Carbon Loss Due to Internal Decay in Living Trees Using Tomography: Implications for Forest Carbon Budgets. *Environ. Res. Lett.* **2018**, *13*, doi:10.1088/1748-9326/aae2bf.

25.  Hauck, M.; Csapek, G.; Dulamsuren, C. The Significance of Large Old Trees and Tree Cavities for Forest Carbon Estimates. *For. Ecol. Manage.* **2023**, *546*, 121319, doi:10.1016/j.foreco.2023.121319.

26.  Martin, A.R.; Domke, G.M.; Doraisami, M.; Thomas, S.C. Carbon Fractions in the World's Dead Wood. *Nat. Commun.* **2021**, *12*, 1–9, doi:10.1038/s41467-021-21149-9.

27.  Köster, K.; Metslaid, M.; Engelhart, J.; Köster, E. Dead Wood Basic Density, and the Concentration of Carbon and Nitrogen for Main Tree Species in Managed Hemiboreal Forests. *For. Ecol. Manage.* **2015**, *354*, 35–42, doi:https://doi.org/10.1016/j.foreco.2015.06.039.

28.  Šenhofa, S.; Jaunslaviete, I.; Šņepsts, G.; Jansons, J.; Liepa, L.; Jansons, A. Deadwood Characteristics in Mature and Old-Growth Birch Stands and Their Implications for Carbon Storage. *Forests* **2020**, *11*, 536, doi:10.3390/F11050536.

29.  Stakėnas, V.; Varnagirytė-Kabašinskienė, I.; Sirgedaitė-Šėžienė, V.; Armolaitis, K.; Araminienė, V.; Muraškienė, M.; Žemaitis, P. Dead Wood Carbon Density for the Main Tree Species in the Lithuanian Hemiboreal Forest. *Eur. J. For. Res.* **2020**, *139*, 1045–1055, doi:10.1007/s10342-020-01306-3.

30.  Zabel, R.A.; Morrell, J.J. Decays Originating in the Stems of Living Trees. *Wood Microbiol.* **2020**, 311–337, doi:10.1016/b978-0-12-819465-2.00012-7.

31.  Soge, A.O.; Popoola, O.I.; Adetoyinbo, A.A. Detection of Wood Decay and Cavities in Living Trees: A Review. *Can. J. For. Res.* **2021**, *51*, 937–947, doi:10.1139/cjfr-2020-0340.

32.  Ahti, T.; Hämet-Ahti, L.; Jalas, J. Vegetation Zones and Their Sections in Northwestern Europe. *Ann. Bot. Fenn.* **1968**, *3*, 169–211.

33.  Allikmäe, E.; Laarmann, D.; Korjus, H. Vitality Assessment of Visually Healthy Trees in Estonia. *Forests* **2017**, *8*, doi:10.3390/f8070223.

34.  Liepa, I. *Pieauguma Mācība*; LLU: Jelgava, 1996;

35.  Lundgren, L.N.; Pan, H.; Theander, O.; Eriksson, H.; Johansson, U.; Svenningsson, M. Development of a New Chemical Method for Distinguishing between Betulapendula and Betulapubescens in Sweden. *Can. J. For. Res.* **1995**, *25*, 1097–1102, doi:10.1139/x95-121.

36.  Team, R.C. R: A Language and Environment for Statistical Computing 2022.

37.  Arnqvist, G. Mixed Models Offer No Freedom from Degrees of Freedom. *Trends Ecol. Evol.* **2020**, *35*, 329–335, doi:https://doi.org/10.1016/j.tree.2019.12.004.

38.  Johansson, T. Discolored Stems of 12-63-Year-Old European Aspen (Populus Tremula L.). **2013**.

39.  Arhipova, N.; Gaitnieks, T.; Donis, J.; Stenlid, J.; Vasaitis, R. Decay, Yield Loss and Associated Fungi in Stands of Grey Alder (Alnus Incana) in Latvia. *Forestry* **2011**, *84*, 337–348, doi:10.1093/forestry/cpr018.

40.  Kärki, T.; Maltamo, M.; Eerikäinen, K. Diameter Distribution, Stem Volume and Stem Quality Models for Grey Alder (Alnus Incana) in Eastern Finland. *New For.* **2000**, *20*, 65–86.

41.  Arhipova, N.; Gaitnieks, T.; Donis, J.; Stenlid, J.; Vasaitis, R. Heart-Rot and Associated Fungi in Alnus Glutinosa Stands in Latvia. *Scand. J. For. Res.* **2012**, *27*, 327–336, doi:10.1080/02827581.2012.670727.

42.  Claessens, H.; Oosterbaan, A.; Savill, P.; Rondeux, J. A Review of the Characteristics of Black Alder (Alnus Glutinosa (L.) Gaertn.) and Their Implications for Silvicultural Practices. *Forestry* **2010**, *83*, 163–175, doi:10.1093/forestry/cpp038.

43.  Uri, V.; Kukumägi, M.; Aosaar, J.; Varik, M.; Becker, H.; Soosaar, K.; Morozov, G.; Ligi, K.; Padari, A.; Ostonen, I.; et al. Carbon Budgets in Fertile Grey Alder (Alnus Incana (L.) Moench.) Stands of Different Ages. *For. Ecol. Manage.* **2017**, *396*, 55–67, doi:10.1016/j.foreco.2017.04.004.

44.  Hynynen, J.; Niemistö, P.; Viherä-Aarnio, A.; Brunner, A.; Hein, S.; Velling, P. Silviculture of Birch (Betula Pendula Roth and Betula Pubescens Ehrh.) in Northern Europe. *For. An Int. J. For. Res.* **2010**, *83*, 103–119, doi:10.1093/forestry/cpp035.

45.  Stener, L.G.; Rytter, L.; Jansson, G. Effects of Pruning on Wood Properties of Planted Silver Birch in Southern Sweden. *Silva Fenn.* **2017**, *51*, 1–15, doi:10.14214/sf.1713.

46. Buht, M.; Padari, A.; Aosaar, J.; Varik, M.; Aun, K.; Becker, H.; Kukumägi, M.; Sepaste, A.; Uri, V. Biomass Allocation and Equations for Silver Birch ( Betula Pendula ) and Downy Birch ( Betula Pubescens ) in Estonia. *Scand. J. For. Res.* **2023**, 1–11, doi:10.1080/02827581.2023.2273250.

47. Bleive, A.; Liepins, J.; Liepins, K. Internal Decay Assessment Using Drilling Resistance in Mature Common Alder (Alnus Glutinosa (L.) Gaertn.) Stands. *Res. Rural Dev.* **2022**, *37*, 37–43, doi:10.22616/rrd.28.2022.005.

48. Hiratsuka, Y.; Gibbard, D.A.; Bakowsky, 0.; Maier, G.B. *Classification and Measurement of Aspen Decay and Stain in Alberta*; Edmonton, Alberta, 1990;

49. Arhipova, N.; Gaitnieks, T.; Donis, J.; Stenlid, J.; Vasaitis, R. Butt Rot Incidence, Causal Fungi, and Related Yield Loss in Picea Abies Stands of Latvia. *Can. J. For. Res.* **2011**, *41*, 2337–2345, doi:10.1139/x11-141.

50. Rytter, L. Grey Alder in Forestry: Areview. *Nor. J. Agric. Sci.* **1996**, *24*, 61–78.

51. Wei, Z.; Halik, Ü.; Aishan, T.; Abliz, A.; Welp, M. Spatial Distribution Patterns of Trunk Internal Decay of Euphrates Poplar Riparian Forest along the Tarim River, Northwest China. *For. Ecol. Manage.* **2022**, *522*, 120434, doi:10.1016/j.foreco.2022.120434.

52. Heräjärvi, H.; Junkkonen, R. Wood Density and Growth Rate of European and Hybrid Aspen in Southern Finland. *Balt. For.* **2006**, *12*, 2–8.

53. Heräjärvi, H. Variation of Basic Density and Brinell Hardness within Mature Finnish Betula Pendula and b. Pubescens Stems. *Wood Fiber Sci.* **2004**, *36*, 216–227.

54. Saranpää, P. Wood Density and Growth. In *Wood quality and its biological basis*; John R. Barnett, Jeronimidis, G., Eds.; Blackwell Publishing: USA, 2003; p. 240 ISBN 0849328195.

55. Lachowicz, H.; Bieniasz, A.; Wojtan, R. Variability in the Basic Density of Silver Birch Wood in Poland. **2019**, *53*, 1–13.

56. Liepiņš, J.; Ivanovs, J.; Lazdiņš, A.; Jansons, J.; Liepiņš, K. Mapping of Basic Density within European Aspen Stems in Latvia. *Silva Fenn.* **2017**, *51*, 1–9, doi:10.14214/sf.7798.

57. Liepiņš, J.; Liepiņš, K. Mean Basic Density and Its Axial Variation in Scots Pine, Norway Spruce and Birch Stems. *Res. Rural Dev.* **2017**, *1*, 21–27, doi:10.22616/rrd.23.2017.003.

58. Liepiņš, K.; Liepiņš, J.; Ivanovs, J.; Bārdule, A.; Jansone, L.; Jansons, Ā. Variation in the Basic Density of the Tree Components of Gray Alder and Common Alder. *Forests* 2023, *14*.